Original Research

Deep learning-based reconstruction improves image quality

Xin Huang[1#], Jin Shang[1#], Yao Xiao[1], Wei Hou[1], Guangrui Mu[1], Daliang Li[2], Hua Qian[2], Junying Li[3*]

1 Department of Medical Imaging, The First Affiliated Hospital of Xi'an Jiaotong University, Xi'an, Shaanxi, 710061, China
2 Department of Cardiovascular Medicine, The First Affiliated Hospital of Xi'an Jiaotong University, Xi'an, Shaanxi, 710061, China
3 Obstetrical Department, Hanzhong Central Hospital, Hanzhong, Shaanxi, 723000, China

#Xin Huang and Jin Shang contributed equally to this work

***Corresponding Author:** Junying Li; E-mail: 604611027@qq.com

Abstract

Objective

This study aimed to compare the image quality of filtered back projection (FBP), adaptive statistical iterative reconstruction-Veo (ASIR-V) and the deep learning image reconstruction (DLIR) algorithms in low-dose head CT angiography (CTA).

Methods

This prospective study was conducted on 25 patients undergoing head CTA using a 256-slice CT scanner. Patients received 25 mL of iodine contrast (Iopromide, 370 mg I/mL, 3.0 mL/s). Images were reconstructed using DLIR with high settings (DLIR-H) and medium settings (DLIR-M), FBP, and ASIR-V with a blending factor of 50% (ASIR-V 50%). CT values, standard deviations, signal-to-noise ratios (SNR), and contrast-to-noise ratios (CNR) were measured at the basal ganglia, posterior cranial fossa, center of semiovale, and middle cerebral artery. The edge rise slope (ERS) of the middle cerebral artery rim was measured to assess vessel clarity. Image noise, vessel edge definition, and overall quality were scored on a 5-point scale, while sharpness and clarity were rated on a 4-point scale.

Results

FBP images exhibited the highest image noise, as reflected by SD values. DLIR, especially DLIR-H, showed superior noise reduction compared to ASIR-V 50%. SNR followed this trend: FBP < ASIR-V 50% < DLIR-M < DLIR-H. Spatial resolution, measured by ERS for vessel wall clarity, was higher in DLIR images compared to in ASIR-V 50%. DLIR outperformed conventional iterative algorithms in balancing noise reduction and edge clarity, with both DLIR-M and DLIR-H achieving better subjective scores for noise, edge definition, and sharpness than ASIR-V 50% and FBP.

Conclusion

DLIR in low-dose head CTA could reduces image noise, preserve natural texture, and enhance image clarity compared with ASIR-V and FBP methods.

Keywords: head CT angiography; deep learning image reconstruction; filtered back projection; adaptive statistical iterative reconstruction

Introduction

With advancements in CT technology, head and neck CT angiography (CTA) has been widely used in clinical practice due to its non-invasive nature, high efficiency, and excellent diagnostic sensitivity and specificity[1,2]. However, concerns have emerged regarding radiation exposure, potential carcinogenic risks and kidney damage caused by contrast agents, particularly for patients undergoing repeated scans[3]. As a result, reducing radiation dose and contrast agent volume while maintaining image quality has become a key focus for researchers[4].

Certain anatomical regions, such as the posterior cranial fossa, are particularly prone to beam-hardening artifacts from dense cranial structures, potentially obscuring subtle traumatic lesions[5-7]. Iterative reconstruction (IR) techniques have demonstrated the ability to reduce artifacts and image noise, improving image quality in head CT compared to the commonly used filtered back projection (FBP) method[8,9]. However, under low-dose conditions, IR can compromise spatial resolution, leading to loss of real texture and may introduce unnatural "wax artifacts" as the reconstruction weight increases[10,11].

To achieve high-quality imaging with lower radiation doses, novel reconstruction algorithms have been developed. Artificial intelligence (AI), particularly deep learning, has introduced innovative methods for CT image reconstruction[12]. Deep learning image reconstruction (DLIR), a notable advancement, reduces image noise while preserving resolution, outperforming conventional iterative reconstruction techniques. One example is GE Healthcare's DLIR algorithm (True Fidelity™, Milwaukee), which utilizes a deep neural network (DNN) to correct system defects like beam hardening and scattering[4]. While each reconstruction method has its own advantages, there has been no direct

https://dx.doi.org/10.4314/mmj.v37i2.

comparison of different reconstruction techniques for head CTA imaging.

In this study, we aimed to assess the image quality of low-dose head CTA imaging using different reconstruction algorithms, including conventional FBP, adaptive statistical iterative Reconstruction-Veo (ASIR-V) and deep learning image reconstruction (DLIR) methods. Image evaluation included both objective and subjective assessments.

Methods and Materials

Patient collection

This prospective study was approved by the ethics committee of our hospital (the First Affiliated Hospital of Xi'an Jiaotong University), and all participants provided informed consent. Data were collected from patients who underwent cranial CTA between July and September 2020 at our hospital. Inclusion criteria: patients requiring head CTA. Exclusion criteria: (1) patients with renal insufficiency (glomerular filtration rate < 30 mL/min); (2) patients unable to perform venipuncture; (3) patients with iodine allergies.

Scanning and injection parameters

All patients underwent head CTA using a 256-slice spiral CT scanner (Revolution CT, GE Healthcare, Milwaukee, USA). Contrast agent (Iopromide, 370 mgI/mL) was administered via the median elbow vein, and scans were manually triggered. The scan range extended from the top of the skull to the second cervical vertebra. Scanning parameters were as follows: CM volume, 25 mL; injection rate, 3.0 mL/s; tube voltage, 80 kVp; and noise index (NI), 15. Automatic tube current modulation adjusted to meet the NI setting, followed by an additional 40 mL of saline injected at 4.5 mL/s.

DLIR method

The DLIR method was built upon specific knowledge of the detailed design of the CT system. Model training started with an objective task and selection of the training data, which included the input data to the neural network and the corresponding expected output data. Images reconstructed with the high-dose dataset produce the ground truth. The DLIR method was applied on the low-dose datasets to produce an estimation of the reconstructed images. Since the ground truth was known, it was used as the training target for the deep learning-based reconstruction engine. After the completion of supervised training, the DLIR model had been formulated with all parameters pre-computed and fixed, and was able to generate ground truth equivalent high-quality images based on the low-dose images[13].

Image reconstruction

The original low-dose scan data were reconstructed using four methods: ASIR -V 50%, DLIR with medium settings (DLIR-M) and DLIR with high settings (DLIR-H), and FBP. All reconstruction methods used the same reconstruction parameters. ASIR-V 50% was used as the reference standard for comparison. Image analysis included both objective and subjective evaluations.

Objective evaluation

The reconstructed images were analyzed on a GE Advantage workstation (AW4.7) by two radiologists, each with over 10 years of CT imaging experience. Mean CT values and standard deviations (SD) were measured for the centrum semiovale, basal ganglia, posterior cranial fossa, cervical musculature, and middle cerebral artery. The signal-to-noise ratio (SNR) was calculated as SNR= ROI target/SD target, and the contrast-to-noise ratio (CNR) as CNR = [(ROI vessel – ROI muscle)/SD muscle], using muscle as the background. The region of interest (ROI) areas were 50 mm^2 for the semiovale, basal ganglia, posterior cranial fossa, and cervical musculature, and 2 mm^2 for the middle cerebral artery. The ROI was placed near the center of the vessel, avoiding calcification and plaques. We used the concept of beam hardening artifact (BHA) index introduced by Lin et al[14] to reflect the changes in non-uniformity of CT values caused by beam hardening artifacts. Specifically, the BHA was defined as: BHA = $\sqrt{SD_p^2 - SD_m^2}$,

where SDp^2 represented the SD of the posterior fossa and SDm^2 represented the SD of the neck muscle, used as the background in this study.

Edge rise slope (ERS) was measured using ImageJ software (National Institutes of Health) (http://rsb.info.nih.gov/ij). A straight segment of the middle cerebral artery was selected, and a line was drawn across the vessel lumen from surrounding brain tissue (avoiding calcification and plaque, Figure. 1a, b). The Draw Contour tool in the Analysis tab generated a spatial position curve against CT values. The X-axis represented spatial position, and the Y-axis represented CT value. ERS was calculated to reflect vessel lumen sharpness[15]. ERS is defined as the CT value difference between the last descending point and the first peak on the rapidly ascending curve, divided by the distance between these points (Figure. 1c)[16]. Larger ERS values indicate sharper edges.

Subjective evaluation

Two experienced radiologists, each with over 10 years of head CT imaging experience, independently and blindly evaluated the qualitative image quality. Any disagreements were resolved through discussion to reach a consensus. Image noise was graded on a 5-point scale: Grade 0 (slight), Grade 1 (mild), Grade 2 (moderate), Grade 3 (high), and Grade 4 (severe). Sharpness and clarity were assessed on a 5-point scale: Grade 0 (no blurring), Grade 1 (slightly blurred), Grade 2 (moderately blurred), Grade 3 (highly blurred), and Grade 4 (severely blurred)[17].

Statistical analysis

Statistical analysis was performed using SPSS 22, with measurement data expressed as mean ± standard deviation. Objective measurements (CT value, SD, SNR, and CNR) from the four reconstruction methods (ASIR-V 50%, DLIR-M, DLIR-H, and FBP) were compared using one-way ANOVA, while subjective image quality scores were analyzed using the Kruskal–Wallis test. Consistency was evaluated using the Kappa test, where Kappa values ≥ 0.75 indicated good consistency, 0.4 < Kappa < 0.75 indicated moderate consistency, and Kappa ≤ 0.4 indicated poor consistency. A p-value < 0.05 was considered statistically significant.

Results

Based on the inclusion and exclusion criteria, a total of 25 patients (12 males, 48%), aged 31 to 73 years with a mean age of 55.24 ± 12.91 years, were included. All patients underwent low-dose head CTA. The mean CT dose index (CTDIvol) was (5.69 ± 0.53) mGy, the dose length product (DLP) was (183.72 ± 60.96) mGy·cm-1, and the effective dose (ED) was (0.34 ± 0.16) mSv (Table1).

Table 1 Normal information of low-dose head CTA	
CTDIvol (mGy)	5.69 ± 0.53
DLP (mGy·cm)	183.72 ± 60.96
ED (mSv)	0.34 ± 0.16
CM (mL)	25
Rate (mL/s)	3.0
Tube voltage(kVp)	80
Age (years)	55.24 ± 12.91
Note: CTDIvol: volumetric CT dose index; DLP: measurement length product; ED: effective dose; CM: contrast medium	

Quantitative analysis

The results of the quantitative analysis are presented in Table 2. CT values and standard deviations (SD) were measured for the center of semiovale, basal ganglia, posterior cranial fossa, cervical muscles, and middle cerebral artery, along with calculations for SNR, CNR, and the posterior cranial fossa BHA index. CT values were comparable across all four reconstruction groups. FBP images had the highest SD, while DLIR-H images had the lowest, with SD decreasing as DLIR levels increased. For SNR and CNR, except for the middle cerebral artery, which showed no significant difference ($p > 0.05$), DLIR-H and DLIR-M showed superior values in the other regions ($p < 0.05$). DLIR-M and DLIR-H significantly reduced BHA in the posterior cranial fossa, with lower SD and BHA index values ($p < 0.001$) (Figure 2). Across all ROIs, the SNR and CNR values ranked as follows: DLIR-H > DLIR-M > ASIR-V 50% > FBP. Table 3 shows the ERS results for the four reconstruction methods and pairwise comparisons. The difference in ERS between the DLIR and ASIR-V 50% reconstruction groups was statistically significant, with DLIR-H having the highest mean ERS.

Table 2 Quantitative analysis (objective evaluation)					
	ASIR-V 50%	FBP	DLIR-M	DLIR-H	P value
Centrum semiovale					
HU	32.37 ± 3.65	32.44 ± 3.73	32.49 ± 5.13	32.77 ± 4.08	0.865
SD	11.15 ± 1.73	17.87 ± 2.40	8.73 ± 1.74	6.69 ± 1.12	0.001
SNR	2.96 ± 0.50	1.84 ± 0.28	3.86 ± 0.95	4.75 ± 0.81	0.001
Basal ganglia					
HU	43.06 ± 5.24	43.24 ± 5.80	45.42 ± 4.48	45.75 ± 4.97	0.107
SD	11.63 ± 1.88	18.71 ± 2.96	8.78 ± 1.71	6.65 ± 1.55	0.001
SNR	3.79 ± 0.71	2.36 ± 0.44	5.42 ± 1.47	7.30 ± 2.14	0.001
Middle cerebral artery					
HU	347.75 ± 101.88	348.05 ± 101.63	369.79 ± 82.77	369.63 ± 82.07	0.413
SD	13.70 ± 9.82	17.30 ± 10.02	7.93 ± 3.93	5.44 ± 3.06	0.008
SNR	59.90 ± 37.32	67.25 ± 111.42	106.78 ± 98.70	110.04 ± 134.12	0.061
CNR	48.37 ± 54.08	42.00 ± 52.15	42.94 ± 24.33	48.47 ± 24.90	0.776
Posterior fossa					
HU	48.28 ± 6.75	48.47 ± 7.06	49.84 ± 5.21	49.11 ± 6.07	0.607
SD	14.02 ± 2.19	21.88 ± 3.23	12.06 ± 2.89	9.49 ± 2.32	0.003
BHA	2.11 ± 0.71	2.78 ± 0.75	2.13 ± 0.61	1.80 ± 0.53	0.03
Neck muscles					
HU	59.02 ± 5.25	59.38 ± 5.50	54.88 ± 7.29	56.35±6.27	0.022
SD	10.69 ± 3.45	15.91 ± 4.98	8.06 ± 2.65	6.92 ± 3.50	0.001
Note: Data are presented with mean value ± standard deviation. HU = mean CT number, SD = image noise.					

Figure 2 showed a CTA image from a 71-year-old male, with reconstructions at the centrum semiovale (upper row), basal ganglia (middle row), and posterior cranial fossa (lower row) using FBP, ASIR-V 50%, DLIR-M, and DLIR-H (in that order). Identical-colored boxes indicate the same reconstruction. The FBP images displayed slightly higher noise and significant granularity compared to ASIR-V 50%. DLIR provided lower image noise and improved contrast across all regions, while maintaining a clear and natural image appearance.

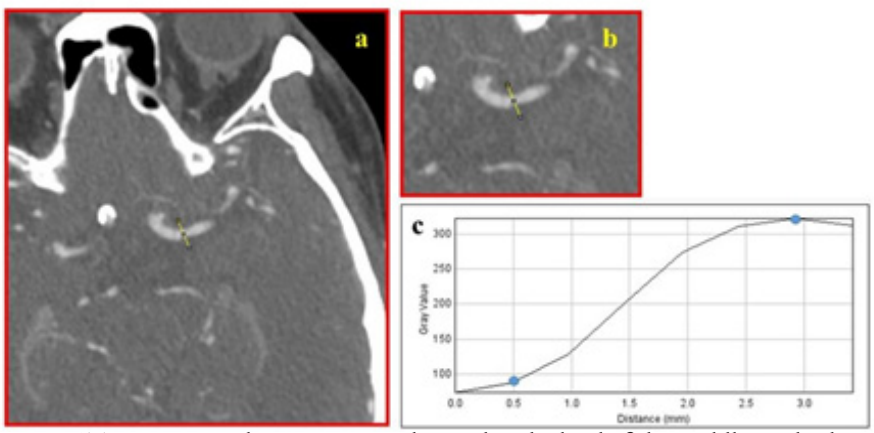

Figure 1 CT attenuation-distance curves obtained at the level of the middle cerebral artery in a 71-year-old male patient (c), where the two blue dots indicate the CT values between the last descent and the first peak on the rapidly rising curve; (a, b) show the measurement method of ERS.

Qualitative evaluation

The results of the subjective qualitative analysis from both radiologists are presented in Table 4 and Figure 3. The two radiologists showed substantial agreement (Kappa value = 0.879). In low-dose imaging, the subjective evaluation

https://dx.doi.org/10.4314/mmj.v37i2.

Table 3 ERS comparison of four reconstruction methods.				
	ASIR-V 50%	FBP	DLIR-M	DLIR-H
ERS (HU/mm)	109.71 ± 33.65	120.32 ± 32.79	123.70 ± 38.83	126.34 ± 37.61
Pairwise comparisons				
ASIR-V50%	--	0.086	0.010	0.016
FBP	--	--	0.624	0.472
DLIR-M	--	--	--	0.621
DLIR-H	--	--	--	--
Note: Data are presented with mean value ± standard deviation.				

Table 4 Qualitative analysis of subjective evaluation					
	ASIR-V 50%	PBP	DLIR-M	DLIR-H	p
Radiologist 1					
Noise	1.72 ± 0.63	3.18 ± 0.59	0.64 ± 0.49	0.23 ± 0.43	< 0.001
Sharpness	22.68 ± 0.65	1.36 ± 0.49	3.36 ± 0.49	3.68 ± 0.48	< 0.001
Radiologist 2					
Noise	1.77 ± 0.53	3.27 ± 0.55	0.64 ± 0.49	0.27 ± 0.46	< 0.001
Sharpness	2.64 ± 0.58	1.27 ± 0.46	3.45 ± 0.51	3.73 ± 0.46	< 0.001
Note: Data are presented with mean value ± standard deviation.					

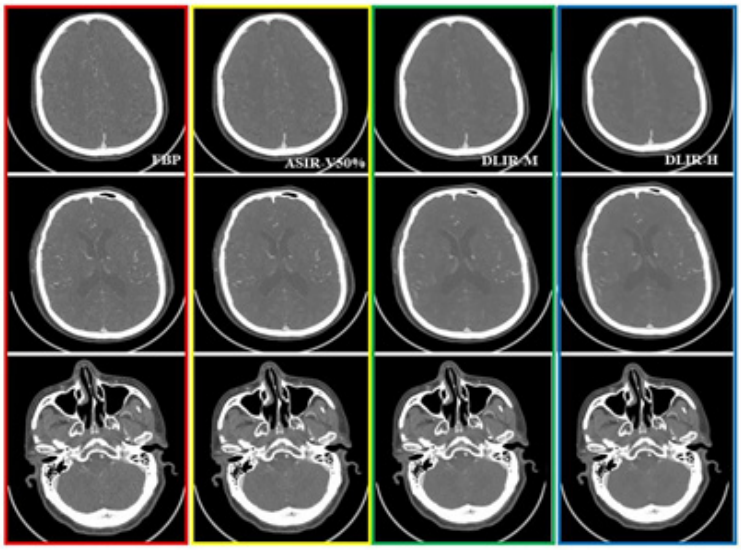

Figure 2 CTA images reconstructed using four methods of the head of a 71-year-old male

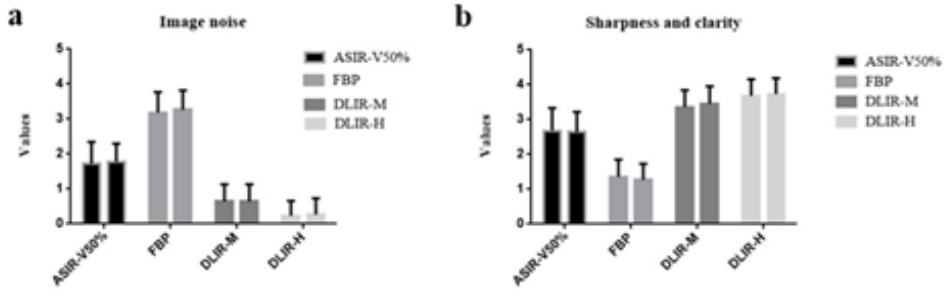

Figure 3 Comparison of image noise (a), sharpness and clarity (b) between the two radiologists

scores indicated a gradual reduction in noise, which improved as DLIR intensity increased. FBP had the highest noise scores (Radiologist 1: 3.18 ± 0.59; Radiologist 2: 3.27 ± 0.55) and the lowest scores for image sharpness and clarity (Radiologist 1: 1.36 ± 0.49; Radiologist 2: 1.27 ± 0.46). The DLIR-H group achieved the highest clarity and sharpness scores. Compared with ASIR-V 50%, DLIR-H showed significant improvements in sharpness ($p < 0.001$ for both radiologists) (Radiologist 1: 3.68 ± 0.48 vs. 2.68 ± 0.65; Radiologist 2: 3.73 ± 0.46 vs. 2.64 ± 0.58). The overall trend in image clarity and sharpness was FBP < ASIR-V 50% < DLIR-M < DLIR-H.

Discussion

In this study, we compared the image quality of DLIR, ASIR-V 50%, and FBP reconstruction algorithms for low-dose head CT angiography. Our findings showed that FBP had the weakest performance in reducing image noise and enhancing sharpness. DLIR exhibited significant advantages in noise reduction, sharpness, and spatial resolution. Compared with ASIR-V 50%, both DLIR-M and DLIR-H significantly improved quantitative image quality, with lower noise levels and higher SNR and CNR. DLIR-H attained the highest overall subjective image quality scores.

Berrington et al.[18] highlighted the risk of radiation-induced cancer. Reducing the radiation dose in head and neck CTA is particularly important due to the large scanning area and the sensitivity of organs such as the lens and thyroid. However, lowering the radiation dose can degrade CT density resolution, increasing noise and affecting lesion detection. Advances in CT imaging hardware and software help compensate for the loss of image quality under low-dose conditions. FBP, which reconstructs images by applying high-pass filters and inverse projection, is fast and stable but produces increased noise, especially in larger patients or low-dose scans[19-21]. IR methods reduce noise, but at high weights, they can introduce blurring artifacts that compromise diagnostic accuracy, and limit their clinical use. Balancing radiation dose reduction with image quality and diagnostic precision remains a challenge. Recently, DLIR has emerged as a promising solution, offering superior noise reduction and improved image quality in low-dose head CT

compared to other reconstruction algorithms[22].

DLIR enhances CT image quality using deep convolutional neural networks (DNNs). Trained on low-dose, high-quality FBP datasets, DLIR efficiently distinguishes between signal and noise, suppressing noise without affecting anatomical or pathological structures[16]. Technical details of the DLIR algorithm (True Fidelity™) are available in the manufacturer's white paper[23]. Alagic Z et al.24 demonstrated that trauma head CT images reconstructed with DLIR, particularly DLIR-H, were superior to those reconstructed with ASIR. Similarly, Nagayama Y et al.[22] found that DLIR provided lower image noise, higher gray-white matter contrast, and improved CNR compared with standard-dose reconstructions. In our study, DLIR significantly reduced noise in the posterior cranial fossa compared with ASIR-V 50%, aligning with findings by Alagic Z et al.[24] in trauma CT scans. Overall, DLIR processing significantly enhanced the image quality of low-dose head CTA.

In our study, we compared the image quality of ASIR-V 50%, DLIR (medium and high levels), and FBP. Image noise, reflected by SD values, was highest in FBP images. DLIR, especially DLIR-H, demonstrated superior noise reduction compared to ASIR-V 50%. SNR followed the trend: FBP < ASIR-V 50% < DLIR-M < DLIR-H. Spatial resolution was objectively assessed using ERS to evaluate vessel wall clarity, with DLIR images showing sharper vessel walls than ASIR-V 50%. DLIR outperformed conventional iterative algorithms in balancing noise and edge clarity, and both DLIR-M and DLIR-H achieved higher subjective scores in image noise, edge definition, and sharpness compared to ASIR-V 50% and FBP.

Our study still has several limitations. First, the small sample size may introduce bias, and future studies should include more cases for further validation. Second, our research focused solely on low-dose imaging; in the future, we plan to introduce a standard-dose group to compare image quality across different reconstruction techniques. Third, we only evaluated three reconstruction algorithms, and future studies will explore additional methods to improve image quality.

Conclusion

In conclusion, our study demonstrated that DLIR preserved image clarity and sharpness in low-dose head CTA compared with the ASIR-V and FBP algorithms, with DLIR-H achieving the highest image quality scores.

Acknowledgements

This work was supported by the Natural Science Foundation of Shaanxi Province (No. 2023-JC-QN-0979).

Funding

This work was supported by the Key Research and Development Projects of Shaanxi Province, China (No. 2025CY-YBXM-196)

Conflicts of interest

The authors declare that they have no known competing financial interests or personal relationships that could have appeared to influence the work reported in this paper.

Data availability statement

The datasets used and analyzed during the current study are available from the corresponding author on reasonable request.

References

1. Wintermark M, Sanelli PC, Anzai Y, Tsiouris AJ, Whitlow CT; ACR Head Injury Institute, et al. Imaging evidence and recommendations for traumatic brain injury: conventional neuroimaging techniques. J Am Coll Radiol. 2015 Feb;12(2):e1-14. doi:10.1016/j.jacr.2014.10.014.

2. Huan Y, Chaoyang Z, Kai D, Chunhua S, Xin Z, Yue Z. Predictive Value of Head-Neck CTA Combined with ABCD2 Scale Score for Patients with Cerebral Infarction of Vertebrobasilar Transient Ischemic Attack (TIA). Med Sci Monit. 2018 Dec 12;24:9001-9006. doi: 10.12659/MSM.909470.

3. Ren Z, Zhang X, Hu Z, Li D, Liu Z, Wei D, et al. Reducing Radiation Dose and Improving Image Quality in CT Portal Venography Using 80 kV and Adaptive Statistical Iterative Reconstruction-V in Slender Patients. Acad Radiol. 2020 Feb;27(2):233-243. doi: 10.1016/j.acra.2019.02.022.

4. Huang X, Zhao W, Wang G, Wang Y, Li J, Li Y, et al. Improving image quality with deep learning image reconstruction in double-low-dose head CT angiography compared with standard dose and adaptive statistical iterative reconstruction. Br J Radiol. 2023 Mar;96(1143):20220625. doi: 10.1259/bjr.20220625.

5. Zacharia TT, Nguyen DT. Subtle pathology detection with multidetector row coronal and sagittal CT reformations in acute head trauma. Emerg Radiol. 2010 Mar;17(2):97-102. doi: 10.1007/s10140-009-0842-6.

6. Bello HR, Graves JA, Rohatgi S, Vakil M, McCarty J, Van Hemert RL, et al. Skull Base-related Lesions at Routine Head CT from the Emergency Department: Pearls, Pitfalls, and Lessons Learned. Radiographics. 2019 Jul-Aug;39(4):1161-1182. doi: 10.1148/rg.2019180118.

7. Pinto P S , Poretti A , Meoded A , Tekes A , Huisman TAGM. The Unique Features of Traumatic Brain Injury in Children. Review of the Characteristics of the Pediatric Skull and Brain, Mechanisms of Trauma, Patterns of Injury, Complications and Their Imaging Findings-Part 1. Journal of Neuroimaging, 2012. doi:10.1111/j.1552-6569.2011.00688.x.

8. Southard RN, Bardo DME, Temkit MH, Thorkelson MA, Augustyn RA, Martinot CA. Comparison of Iterative Model Reconstruction versus Filtered Back-Projection in Pediatric Emergency Head CT: Dose, Image Quality, and Image-Reconstruction Times. AJNR Am J Neuroradiol. 2019 May;40(5):866-871. doi: 10.3174/ajnr.A6034.

9. Rivers-Bowerman MD, Shankar JJ. Iterative Reconstruction for Head CT: Effects on Radiation Dose and Image Quality. Can J Neurol Sci. 2014 Sep;41(5):620-5. doi: 10.1017/cjn.2014.11.

10. Samei E, Richard S. Assessment of the dose reduction potential of a model-based iterative reconstruction algorithm using a task-based performance metrology. Med Phys. 2015 Jan;42(1):314-23. doi: 10.1118/1.4903899.

11. Park HJ, Choi SY, Lee JE, Lim S, Lee MH, Yi BH, et al. Deep learning image reconstruction algorithm for abdominal multidetector CT at different tube voltages: assessment of image quality and radiation dose in a phantom study. Eur Radiol. 2022 Jun;32(6):3974-3984. doi: 10.1007/s00330-021-08459-8.

12. Zhang Z, Seeram E. The use of artificial intelligence in computed tomography image reconstruction - A literature review. J Med Imaging Radiat Sci. 2020 Dec;51(4):671-677. doi: 10.1016/j.jmir.2020.09.001.

13. Hsieh, J., Liu, E., Nett, B., Tang, J., Thibault, J. B., & Sahney, S. (2019). A new era of image reconstruction: TrueFidelity™. White Paper (JB68676XX), GE Healthcare.

14. Lin XZ, Miao F, Li JY, Dong HP, Shen Y, Chen KM. High-definition CT Gemstone spectral imaging of the brain: initial results of selecting optimal monochromatic image for beam-hardening artifacts and image noise reduction. J Comput Assist Tomogr. 2011 Mar-Apr;35(2):294-7. doi: 10.1097/RCT.

15. Suzuki S, Machida H, Tanaka I, Ueno E. Vascular diameter

measurement in CT angiography: comparison of model-based iterative reconstruction and standard filtered back projection algorithms in vitro. AJR Am J Roentgenol. 2013 Mar;200(3):652-7. doi: 10.2214/AJR.12.8689.

16. Qu T, Guo Y, Li J, Cao L, Li Y, Chen L, et al. Iterative reconstruction vs deep learning image reconstruction: comparison of image quality and diagnostic accuracy of arterial stenosis in low-dose lower extremity CT angiography. Br J Radiol. 2022 Dec 1;95(1140):20220196. doi: 10.1259/bjr.20220196.

17. Park C, Choo KS, Kim JH, Nam KJ, Lee JW, Kim JY. Image Quality and Radiation Dose in CT Venography Using Model-Based Iterative Reconstruction at 80 kVp versus Adaptive Statistical Iterative Reconstruction-V at 70 kVp. Korean J Radiol. 2019 Jul;20(7):1167-1175. doi: 10.3348/kjr.2018.0897.

18. Berrington de González A, Darby S. Risk of cancer from diagnostic X-rays: estimates for the UK and 14 other countries. Lancet. 2004 Jan 31;363(9406):345-51. doi: 10.1016/S0140-6736(04)15433-0.

19. Iezzi R, Santoro M, Marano R, Di Stasi C, Dattesi R, Kirchin M, et al. Low-dose multidetector CT angiography in the evaluation of infrarenal aorta and peripheral arterial occlusive disease. Radiology. 2012 Apr;263(1):287-98. doi: 10.1148/radiol.11110700.

20. Qian WL, Zhou DJ, Jiang Y, Feng C, Chen Q, Wang H, et al. Ultra-low radiation dose CT angiography of the lower extremity using the iterative model reconstruction (IMR) algorithm. Clin Radiol. 2018 Nov;73(11):985.e13-985.e19. doi: 10.1016/j.crad.2018.08.001.

21. Keller G, Götz S, Kraus MS, Grünwald L, Springer F, Afat S. Radiation Dose Reduction in CT Torsion Measurement of the Lower Limb: Introduction of a New Ultra-Low Dose Protocol. Diagnostics (Basel). 2021 Jul 3;11(7):1209. doi: 10.3390/diagnostics11071209.

22. Nagayama Y, Iwashita K, Maruyama N, Uetani H, Goto M, Sakabe D, et al. Deep learning-based reconstruction can improve the image quality of low radiation dose head CT. Eur Radiol. 2023 May;33(5):3253-3265. doi: 10.1007/s00330-023-09559-3

23. Healthcare GE. A new era of image reconstruction: TrueFidelity; 2019.

24. Alagic Z, Diaz Cardenas J, Halldorsson K, Grozman V, Wallgren S, Suzuki C, et al. Deep learning versus iterative image reconstruction algorithm for head CT in trauma. Emerg Radiol. 2022 Apr;29(2):339-352. doi: 10.1007/s10140-021-02012-2.